STATE-OF-THE-ART REVIEW

Clinical Phenotypes of Heart Failure With Preserved Ejection Fraction to Select Preclinical Animal Models

Willem B. van Ham, MSc,[a],* Elise L. Kessler, PhD,[b,c],* Marish I.F.J. Oerlemans, MD, PhD,[d] M. Louis Handoko, MD, PhD,[e] Joost P.G. Sluijter, PhD,[b,c] Toon A.B. van Veen, PhD,[a] Hester M. den Ruijter, PhD,[b] Saskia C.A. de Jager, PhD[b]

HIGHLIGHTS

- To better define HFpEF clinically, patients are nowadays often clustered into phenogroups, based on their comorbidities and symptoms
- Many animal models claim to mimic HFpEF, but phenogroups are not yet regularly used to cluster them
- HFpEF animals models often lack reports of clinical symptoms of HF, therefore mainly presenting as extended models of LVDD, clinically seen as a prestate of HFpEF
- We investigated if clinically relevant phenogroups can guide selection of animal models aiming at better defined animal research

SUMMARY

At least one-half of the growing heart failure population consists of heart failure with preserved ejection fraction (HFpEF). The limited therapeutic options, the complexity of the syndrome, and many related comorbidities emphasize the need for adequate experimental animal models to study the etiology of HFpEF, as well as its comorbidities and pathophysiological changes. The strengths and weaknesses of available animal models have been reviewed extensively with the general consensus that a "1-size-fits-all" model does not exist, because no uniform HFpEF patient exists. In fact, HFpEF patients have been categorized into HFpEF phenogroups based on comorbidities and symptoms. In this review, we therefore study which animal model is best suited to study the different phenogroups—to improve model selection and refinement of animal research. Based on the published data, we extrapolated human HFpEF phenogroups into 3 animal phenogroups (containing small and large animals) based on reports and definitions of the authors: animal models with high (cardiac) age (phenogroup aging); animal models focusing on hypertension and kidney dysfunction (phenogroup hypertension/kidney failure); and models with hypertension, obesity, and type 2 diabetes mellitus (phenogroup cardiometabolic syndrome). We subsequently evaluated characteristics of HFpEF, such as left ventricular diastolic dysfunction parameters, systemic inflammation, cardiac fibrosis, and sex-specificity in the different models. Finally, we scored these parameters concluded how to best apply these models. Based on our findings, we propose an easy-to-use classification for future animal research based on clinical phenogroups of interest. (J Am Coll Cardiol Basic Trans Science 2022;7:844–857) © 2022 The Authors. Published by Elsevier on behalf of the American College of Cardiology Foundation. This is an open access article under the CC BY-NC-ND license (http://creativecommons.org/licenses/by-nc-nd/4.0/).

From the [a]Department of Medical Physiology, University Medical Center Utrecht, Utrecht, the Netherlands; [b]Laboratory for Experimental Cardiology, Department of Cardiology, University Medical Center Utrecht, Utrecht, the Netherlands; [c]Utrecht Regenerative Medicine Center, Circulatory Health Laboratory, University of Utrecht, Utrecht, the Netherlands; [d]Department of Cardiology, University Medical Center Utrecht, Utrecht, the Netherlands; and the [e]Department of Cardiology, Amsterdam University Medical Center, Vrije Universiteit Amsterdam, Amsterdam, the Netherlands. *Drs van Ham and Kessler contributed equally to this work and are joint first authors.

pproximately 50% of the heart failure population is experiencing heart failure with preserved ejection fraction (HFpEF).[1,2] HFpEF is characterized by heart failure (HF) symptoms in addition to structural and functional alterations and a preserved left ventricular ejection fraction (LVEF) (>50%).[3-9] Clinically, patients are often women presenting with congestion, increased levels of natriuretic peptides, and left ventricular diastolic dysfunction (LVDD).[10] Comorbidities like hypertension, obesity, type 2 diabetes mellitus (T2DM), and kidney dysfunction increase morbidity and mortality,[3,6,8,11] which have been associated with systemic inflammation affecting cardiac and vascular structure and function.[9,12,13] This phenotypical heterogeneity hampers finding suitable therapeutical approaches; therefore, diagnostic criteria scores have been developed, such as the H2FPEF[14] and HFA-PEFF,[15] which can be used to identify HFpEF. Besides that, HFpEF patients are nowadays often further defined into so-called phenogroups[16-19] based on severity of LVDD, presence of single or multiple comorbidities, and age to reduce heterogeneity in clinical trials.

To investigate the pathophysiology of HFpEF, animal models are widely used.[20,21] However, the phenotypical heterogeneity within the human patient population cannot be translated to a "1-size-fits-all" animal model. Currently, clinical phenogroups or scores are not regularly used for clustering of animal models, as Withaar et al[22] were the first to attempt this in mice. Their conclusion was that the complex HFpEF pathophysiology in humans has to be taken into account when creating and validating HFpEF animal models.[22] However, several parameters cannot be directly translated from humans to (small) animals, and by defining more suitable phenogroups in animal models, these models can be further refined allowing more precise comparisons between animals and specific phenotypically different patient populations.[23] Therefore, adapted phenoclustering to animal models might improve both fundamental and preclinical research, thereby aiding to better understanding of this complex syndrome.

In this review, we therefore classified animal models to clinical phenogroups of HFpEF to facilitate investigation of pathological mechanisms of LVDD in animal models.

CRITERIA AND REQUIREMENTS FOR PRECLINICAL HFpEF MODELS

We classified preclinical models based on the requirements of clinical HFpEF, as defined by inclusion and exclusion criteria depicted in **Figure 1** and in the following text. A full overview of all characteristics measured in animal models are summarized in Supplemental Table 1 for small animals and Supplemental Table 2 for large animals. Inclusion criteria were HF symptoms, presentation with parameters of LVDD, and structural and functional alterations (such as chronic systemic inflammation and fibrosis) accompanying the development of the syndrome in humans. Exclusion criteria were systolic dysfunction and a reduced ejection fraction (EF). Based on the lack of HF symptoms, one might conclude that most HFpEF animal models are rather extended LVDD models.
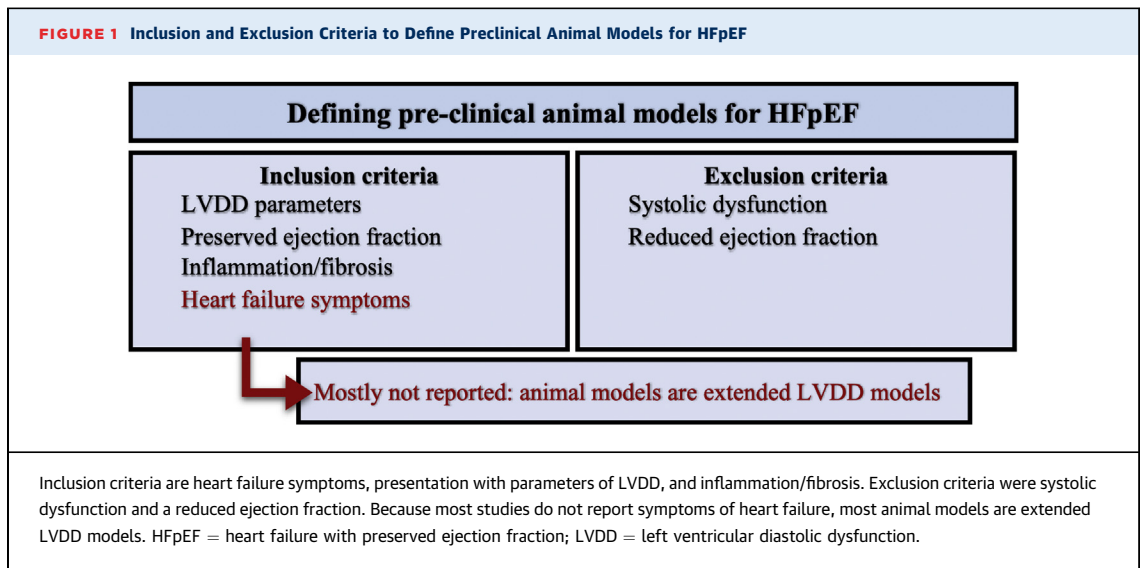
INCLUSION CRITERIA. Left ventricular diastolic dysfunction. Even though currently no guidelines exist to define LVDD for animal models, we think all animals should present with characteristics of LVDD and a clear definition of LVDD should be used to evaluate animal models.

In general, parameters to measure left ventricular (LV) diastolic function in humans and animals are the ratio between mitral peak velocity of early filling to early diastolic mitral annular velocity (E/e' ratio), and the ratio between mitral peak velocity of early filling to mitral peak velocity of late filling (E/A ratio).[24-26] As both can be measured using Doppler ultrasound, this is implemented in many animal studies. Normal values of E/e' and E/A range from 10-16 and 1-2.5 in different animals (Supplemental Tables 1 and 2).[21,27] Elevated E/e' and diminished E/A ratios can depict worsened LV diastolic function. LV active relaxation time (isovolumetric relaxation time [IVRT]), or its constant τ (tau), are indicators for LVDD, but are generally only used in animals.[28] Normally, τ ranges from 20-30 milliseconds in large animals, and from 4-7 and 8-12 milliseconds in mice and rats, respectively (Supplemental Tables 1 and 2).[21] Alternatively, dP/dt$_{min}$ can be determined as a parameter for active

FIGURE 1 Inclusion and Exclusion Criteria to Define Preclinical Animal Models for HFpEF

Defining pre-clinical animal models for HFpEF

Inclusion criteria
LVDD parameters
Preserved ejection fraction
Inflammation/fibrosis
Heart failure symptoms

Exclusion criteria
Systolic dysfunction
Reduced ejection fraction

Mostly not reported: animal models are extended LVDD models

Inclusion criteria are heart failure symptoms, presentation with parameters of LVDD, and inflammation/fibrosis. Exclusion criteria were systolic dysfunction and a reduced ejection fraction. Because most studies do not report symptoms of heart failure, most animal models are extended LVDD models. HFpEF = heart failure with preserved ejection fraction; LVDD = left ventricular diastolic dysfunction.

relaxation. Increased τ, IVRT, or dP/dt$_{min}$ corresponds to a slower LV cardiomyocyte relaxation and therefore increased LV filling time.[26] Recently, LV peak untwist velocity was proposed as an early detectable LVDD parameter in large animals.[29]

In clinical practice, LV hypertrophy is validated by echocardiography and electrocardiography, eg, LV heart weight, LV posterior wall (LVPWd) thickness, and diameter of the interventricular septum (IVSd). In animals, individual cardiomyocyte size and LV weight are often additive measures (ex vivo).[25] Although brain natriuretic peptide (BNP) values are not always increased, they sometimes are used as a hypertrophy blood biomarker.[30] Elevated left ventricular end-diastolic pressure (LVEDP) is a sign of compensation to preserve LVEF,[24] and in most healthy animals, LVEDP is <12 mm Hg. A more recent parameter for LVDD in patients is a decreased left atrial strain, which can also be used to indicate severity of LVDD.[31] Although left atrial volume is sometimes also assessed in animals, changes occur often only after longer periods of remodeling.

Chronic systemic inflammation and fibrosis formation. LVDD and HFpEF patients often experience chronic systemic inflammation, at least partially caused by comorbidities.[9,12,32] Especially in elderly obese women, systemic inflammation is prominent.[33] Both in clinical studies and animal models, inflammatory cells (CD3$^+$, CD45$^+$, and CD68$^+$-positive cells),[34] circulation of inflammatory cytokines (eg, tumor necrosis factor alpha, interleukin-1 and -6), and production of monocyte chemoattractant protein 1 (MCP1) have been measured (Supplemental Tables 1 and 2). Although C-reactive protein values can also

be measured as they are generally upregulated in the pro-inflammatory state, it should be noted that 40% of HFpEF patients have normal C-reactive protein values.[35]

Consequential to the active inflammatory state, eg, increased fibroblast activity caused by MCP-1,[9] LVDD and HFpEF patients experience increased myocardial fibrosis.[36,37] In humans, fibrosis is measured by cardiac cardiac magnetic resonance, specifically T$_1$ mapping.[38] In animal models, it can be measured by increased levels of transforming growth factor beta, collagen I and III, and elevated matrix metalloproteinases (MMPs).[36,39-42] Fibrosis formation can also be detected by postmortem tissue stainings, such as Masson's trichrome or Picro Sirius Red. In patients and animals, both protein and mRNA levels of the inflammatory and fibrotic markers are highly upregulated.[40,43] In general, most models included in the proposed compass have a reasonable assessment of systemic inflammation and myocardial fibrosis.

SYMPTOMS OF HF. Diagnosing HF in animals is hampered by the cumbersome detection of symptoms and signs, but attempts are made, eg, measuring pulmonary edema/congestion (increased lung weight), presence of cachexia, and exercise tolerance or fatigue (based on treadmill or swimming experiments). However, in larger animals this can be more complex, because extensive equipment is needed.[44] Exercise intolerance is considered the best way to detect HF in animal models of HFpEF. Although it is difficult to standardize exercise experiments in animals and to extrapolate these interventions to humans, several models have already evaluated exercise intolerance successfully (reviewed by Valero-Muñoz et al[45]).

FIGURE 2 Classification and Scoring of Animal Models of Heart Failure With Preserved Ejection Fraction

Schematic overview of small and large animal models, visualizing the presence or absence of comorbidities, systemic inflammation, cardiac fibrosis, and left ventricular diastolic dysfunction (LVDD) parameters, using color coding. Phenogroup aging contains the senescence-accelerated mouse prone 8 mouse (SAMP8), as well as the Fischer 344 rat, the hypertrophic heart rat (HHR), and the old hypertensive dog (OHT). Phenogroup hypertension/kidney dysfunction consists of the left ventricular pressure overload pig (LVPO), the pressure overload cat (PO), the angiotensin II mouse (ANGII), the Dahl salt-sensitive rat (DahlSS), the Nω-nitrol-arginine methyl ester mouse (L-NAME), the subtotal nephrectomy rat (SNX), and the deoxycorticosterone acetate rat (DOCA). Phenogroup cardiometabolic syndrome consists of the Zucker diabetic fatty rat (ZDF), the obese mouse (ob/ob), the diabetic mouse (db/db), the high-fat-high-sugar mouse (HFHS), the old high-fat diet + angiotensin II mouse (Old HFD+ANGII), the high-fat-high-sugar pig (HFHS), the Dahl salt sensitive/obese rat (DahlSS/obese), the Zucker fatty and spontaneously hypertensive rat (ZSF1/obese), the Nω-nitrol-arginine methyl ester + high fat diet mouse (L-NAME+HFD), the deoxycorticosterone acetate/angiotensin II/Western diet pig (DOCA/ANGII/WD), the hypertensive, hypercholesterolemia, diabetes mellitus pig (HT/HC/DM), the Western diet/aortic block pig (WD/AB), the diabetic + angiotensin II mouse (db/db+ANGII), and the deoxycorticosterone acetate/Western diet pig (DOCA/WD). Color coding shows whether certain parameters are present and used to score: **dark green** 2 points, **light green** 1 point, **yellow** 0 points, **light green** −1 point, and **dark red** −2 points. Sex differences were not included in scoring. EDPVR = end-diastolic pressure volume relationship; IVRT = isovolumetric relaxation time; LVEDP = left ventricular end-diastolic pressure; LVEF = left ventricular ejection fraction; Ms = mouse; P = pig; PUV = peak untwist velocity; T2DM = type 2 diabetes mellitus (T2DM).

As many animal models are still missing consistent evaluation of clinical symptoms of HF (Figure 1), we concluded that most animal models are rather extended LVDD models than HFpEF models, and therefore mainly focused on the development of LVDD and comorbidities.

CRITERIA TO EXTRAPOLATE CLINICAL PHENOGROUPS INTO PRECLINICAL RESEARCH

Lately, to better define the human HFpEF population, disease patterns like clinical, echocardiographic, and laboratory variables, as well as treatment history and mortality, were used to cluster patients into 2-6 separate phenogroups.[16-19,46-50] Although phenogroups might differ between clinical cohorts, often age, hypertension, kidney dysfunction, and metabolic comorbidities, such as obesity and T2DM, are used to cluster patients, as well as the presence of LVDD.

Based on important characteristics in small and large animal models, we defined 3 phenogroups best reflecting the human phenogroups, based on reports and definitions of parameters by the authors of the original publications: animal models with high age or age-related characteristics (phenogroup aging); animal models focusing on hypertension and kidney dysfunction (phenogroup hypertension/ kidney failure); and models with hypertension, obesity, and T2DM (phenogroup cardiometabolic syndrome).

PHENOGROUP AGING. In the clinical setting, age is an important factor, because HFpEF patients are relatively old with minor differences between the human phenogroups. In animal models, aging alone is almost never an independently investigated characteristic, but mainly together with comorbidities.[51-54] (Cardiac) aging characteristics could without a doubt lead to development of LVDD symptoms, as also seen in the hypertrophic heart rat (HHR) model (55). Including older animals with or without additional comorbidities, or using young animals with a longer follow-up should be considered to further refine the LVDD and HFpEF models.

PHENOGROUP HYPERTENSION/KIDNEY DYSFUNCTION. Hypertension. Hypertension is present in most HFpEF patients (91% in women and 85% in men),[23,56-59] and was therefore required to be present or at least minimally developing in all 3 phenogroups. Hypertension leads to angiotensin II (ANGII)-induced inflammation of the cardiac muscle,[60] and therefore an increased LVEDP, microvascular dysfunction, and increased reactive oxygen species (ROS) production. This is followed by a decrease in nitric oxide (NO), resulting in a less compliant LV and its microvessels,[32,61,62] which can in turn trigger myocardial fibrosis and stiffening.[12]

Hypertension can be triggered in animals, just like in humans, by various factors, ie, high-salt diet and high blood pressure-inducing drugs. In animals, it can be measured by systolic blood pressure or mean arterial pressure, with systolic blood pressure >130 mm Hg, as opposed to ±120 mm Hg in healthy small and large animals (Supplemental Tables 1 and 2).[63-65]

Kidney dysfunction. Kidney dysfunction is present in 30%-50% of the HFpEF patients[4,56,57,66] and is associated with increased mortality.[4,11] It is caused by chronically increased blood pressure (BP), chronic systemic inflammation, and/or metabolic disorders. Kidney dysfunction manifests itself by a compromised filtration of blood and the presence of uremic toxins in the circulation.[67] Elevated production of ROS, via NADPH oxidases, consequential to kidney dysfunction also results in kidney fibrosis formation, additional proinflammatory responses, and further deterioration of kidney function.[68,69]

In humans, the estimated glomerular filtration rate, creatinine clearance, proteinuria, and presence of uremic toxins (UTs), eg, indoles and phenols, are used to measure degree of kidney dysfunction.

In animals, kidney dysfunction can be introduced using high-salt diets or partial nephrectomy, and additional postmortem histological analyses can be performed to investigate glomerulosclerosis or kidney fibrosis.[70-72] Compared with healthy animals, murine and rat kidney dysfunction models show a 3-fold lower creatinine clearance of around 50 μL/min and <150 μL/min, respectively.[73,74] Creatinine clearance in healthy large animals is relative to their age and size, with a clearance of ±100 mL/min in ±60 kg pigs, and ±50 mL/min in ±10 kg dogs.[75,76]

PHENOGROUP CARDIOMETABOLIC SYNDROME. Obesity and diabetes mellitus type 2. About 30%-50% of HFpEF patients present with obesity,[4,23,56,66] with a higher prevalence in women than men.[11,59] Next to that, about 30%-40% of male and female HFpEF patients experience T2DM,[23,57-59] which has been connected to increased LVEDP, and myocardial stiffness caused by titin hypophosphorylation,[77] as well as increased mortality.[78] T2DM is often seen in combination with obesity. Obesity induces systemic inflammation and release of aldosterone leading to microvascular dysfunction and cardiac fibrosis.[3,79] Obesity has also been connected to decreased cyclic guanosine monophosphate levels, causing a lower activity of protein kinase G.

Diminished protein kinase G-dependent titin phosphorylation increases resting cardiomyocyte tension.[80] In animals, obesity is triggered by a high-fat diet (HFD), indicated by triglyceride levels of at least >100 mg/dL.[81] In humans, body weight, body mass index, and waist-to-hip ratio are parameters to measure obesity. In animals, triglyceride levels and cholesterol levels can also be measured, although these are less defined and highly deviating based on age, strain, and sex of the animal.

Both in humans and animal models, measurements of blood glucose or insulin levels are established methods to indicate T2DM. Healthy fasting glucose levels are comparable in small and large animals (80-100 mg/dL).[82-86] T2DM is ascertained at glucose levels of >125 mg/dL in large animals,[84-86] whereas small animals are more tolerant with >150/200 mg/dL as being considered diabetic.[82,83]

EVALUATION OF ANIMAL MODELS BASED ON PHENOGROUPS

We first evaluated an extensive list of currently used animal models with most reported parameters and their pathological *vs* control values. Here, we based our criteria for the HFpEF phenogroups on the self-reported definitions by the authors, because animal models and used read-outs are variable. A full overview of characteristics, (sex; age; LV diastolic function parameters [eg, LVEF, relaxation time, E/A]; pressure parameters; cardiomyocyte size; BNP values; inflammatory, fibrotic, and microvessel dysfunction parameters; blood pressure; body weight; and parameters for glucose and kidney dysfunction, as well as parameters for congestion) are summarized in Supplemental Table 1 for small animals and Supplemental Table 2 for large animals. If multiple studies investigated the same animal model, all of them were used to assess and classify the model. We then extracted the most suitable animal models per phenogroup based on definitions and reports given by the authors of the models regarding inflammation, cardiac fibrosis, LVDD parameters, sexes included, and HFpEF markers as depicted in Figure 2. Because clinical symptoms of HFpEF are not consistently or only partly investigated in animal models, we focused on mechanistic models of extended LVDD. The color-coding is guidance based on (significant) differences of these parameters between animals with pathological conditions and control subjects: green means the characteristic is present; red means the characteristic is absent; and yellow means the characteristic was not assessed or is undefined. The lighter colors (red and green) mean that additional validation of the

parameter by other groups is required. Similar color-coding is used for the column LVDD, based on the presence of at least 3—both structural and functional—parameters of LVDD. Even though we based our decisions on the definitions and reports of the authors of the original publication, we additionally argued that a suitable animal model had to contain the following: 1) a description of multiple parameters defining LVDD, including active and passive relaxation, pressure changes, and structural adaptations; 2) a description of systemic inflammation and the progression of myocardial fibrosis, as both are indicative for LVDD/HFpEF[13,87]; 3) a comorbidity reported to trigger LVDD, such as hypertension or T2DM; and 4) the potential development of other comorbidities, which should also be evaluated in a suitable animal model for the corresponding phenogroup. To be included in the selection, the model had to assess all characteristics over time, to provide information on LV deterioration and the time window of HFpEF development. When characteristics were investigated in more detail or repetitively, reproducibility increased. All parameters underlying our scoring are explained in the following sections.

PHENOGROUPING AND SCORING OF ANIMAL MODELS

In most animal models, hypertension, obesity, and T2DM are used to initiate the development of LVDD, as they are the most common comorbidities in HFpEF patients. Kidney dysfunction often develops spontaneously in animal models, except in the induced deoxycorticosterone acetate (DOCA) and subtotal nephrectomy rats. In most studies, only a single sex was analyzed, and in some of them, the sex of the animals was not specified. We extracted suitable animal models that met our requirements from the extensive list and sorted them into 3 phenogroups based on age, comorbidities, inflammation, cardiac fibrosis, and LV function of the models (Figure 2). Thereafter, we scored selected animal models and drew conclusions on the most suitable animal models for LVDD/HFpEF research relating the 3 phenogroups. Models were scored using an average of 6 groups of characteristics, namely inflammation, fibrosis, LVEF, relaxation parameters, pressure measurements, and structural adaptations, calculated by scoring the color coding (dark green 2 points, light green 1 point, yellow zero points, light red −1 points, and dark red −2 points).

To be scored as an HFpEF model, HF markers had to also be present; however, this was excluded from the scoring because those were not consistently reported. Models that scored high and reported on HF

markers were therefore additionally called HFpEF models. Due to poor reporting of the sex used, it was excluded in the scoring. It is striking, though, that models that scored best also often investigated sex differences already.

PHENOGROUP AGING. Animal models in this phenogroup were mainly aging models or LVDD models induced by cardiac aging-related characteristics (Figure 2, upper panel).

Models that primarily focus on aging are the senescence-accelerated mouse prone 8 mouse and the Fischer 344 rat. Although the senescence-accelerated mouse prone 8 mouse model develops kidney dysfunction,[51,52] the Fischer 344 rat only develops hypertension.[53,54] Both animal models provisionally miss measurements to assume development of LVDD, but represent the older age and age-related structural alterations. In the HHR,[55] no comorbidities were used to trigger LVDD and insights in comorbidities or systemic inflammation were absent, even though LVDD was demonstrated quite extensively and reproducibility was shown. The old hypertensive (OHT) dog,[88-91] induced by renal-wrapping, is also a model of hypertension in old animals, which scored best based on our scoring.

PHENOGROUP HYPERTENSION/KIDNEY DYSFUNCTION. Animal models were included in this phenogroup if they presented with hypertension and kidney dysfunction or developed hypertension by alterations in ANGII, high-salt diet, or L-NAME (Figure 2, middle panel).

In the LV pressure overload (PO) pig[92-94] and the PO cat,[95,96] LVDD was demonstrated and reproducible. The ANGII mouse[97-100] or the DahlSS rat[101-104] are both established hypertensive LVDD/HFpEF animal models, which potentially develop kidney dysfunction. Recently, the DahlSS model was investigated in male and female rats separately, which showed less fibrosis in female mice and excessive weight loss in male mice.[104] Also L-NAME administration in mice was introduced as a potential inducer of hypertension.[105,106]

The subtotal nephrectomy rat is used to investigate the development of LVDD specifically upon kidney dysfunction, without development of systemic inflammation.[107,108] Interestingly, despite almost all functional parameters significantly pointing toward LVDD, this model has rarely been used for LVDD/HFpEF research specifically, presumably caused by being on the edge of diastolic to systolic dysfunction. In parallel, more research focusing on cardiac adaptations and fibrosis formation is required in these hypertensive models. The DOCA rat is based on uninephrectomy, but the additional DOCA salt administration also shifts the pathological focus on progressive hypertension.[109-111] These models can be used to investigate hypertension-induced vascular dysfunction suggested to be prominent in this phenogroup.[18]

In conclusion, the most promising small animal models are the ANGII mouse and the DahlSS rat, where both models also investigated HF markers. Also, the DOCA rats are scoring well for LVDD, because they develop hypertension and kidney dysfunction. The LVPO was the highest scoring large animal model with no underlying comorbidities, but presence of systemic inflammation, fibrosis, and LVDD parameters.

PHENOGROUP CARDIOMETABOLIC SYNDROME. Comparable to the clinical phenogroup, the phenogroup cardiometabolic syndrome includes mainly animal models with a large number (>2) of comorbidities (Figure 2, lower panel).

The Zucker diabetic fatty rat[112-114] model is a T2DM model with compensatory cardiac hypertrophy and increased LVEDP, but requires more research into other LVDD parameters. Obese (ob/ob)[115-118] and diabetic (db/db)[119-122] mice are both established models for the combination of obesity and T2DM, with changes in all indicated LVDD parameters in db/db mice, but no cardiac fibrosis formation in ob/ob mice. In both models, male and female mice were studied separately, without significant sex differences. A model of diabetic cardiomyopathy is the HFHS mouse,[123] which displays LVDD and 3 worsened parameters, inflammation, and cardiac fibrosis. Hypertension, obesity, T2DM, as well as inflammation and cardiac fibrosis are shown in the old HFD + ANGII mouse, without the presence of kidney dysfunction.[124] The HFHS pig[125] is a potential metabolic model for early LVDD, investigated by peak untwist velocity.

DahlSS/obese[72,126,127] and Zucker fatty and spontaneously hypertensive (ZSF1)/obese rats[62,70,128] describe a combination of hypertension and metabolic disorder. Both develop LVDD, indicated by 5 and 6 parameters, respectively. Aside from the induced hypertension and obesity/T2DM, inflammation, fibrosis, and kidney dysfunction were reported. High mortality rates after 15 weeks often hamper extending the experimental timeline. The L-NAME + HFD mouse models also shows 4 LVDD parameters, but without the presence of T2DM.[105,106] The same phenotype is described in the DOCA + ANGII + western diet (WD) pig[129], which describes all LVDD parameters, but reproducibility is needed. The hypertensive, hypercholesterolemia, and diabetes mellitus (HT/HC/DM) pig[12,130] and WD + aortic block (AB) pig[131] both include the broad

pathological spectrum of all comorbidities of LVDD and HFpEF. Whereas in the HT/HC/DM model, relaxation abnormalities are investigated more cellularly, the WD + AB model showed LVDD in all functional parameters.

Some animal models were not described in detail or did not have LVDD or HFpEF as the main outcome, eg, the db/db + ANGII mouse[132] and DOCA + WD pig.[71] Both models had no relaxation alterations and did not prove LVDD, leaving it undetermined if any pathological HFpEF phenotype were present, while insights into all comorbidities were included.

For this phenogroup, the db/db mice, DahlSS/obese and ZSF1/obese rats, and HT/HC/DM pig scored best, all for which HF markers have been shown. Despite lower scores, the DOCA + ANGII + WD and the WD + AB pig models fit the phenogroup, as LVDD was proven most extensively.

DISCUSSION

ADVANTAGES OF CLUSTERING ANIMAL MODELS.
Although strengths and weaknesses of individual LVDD/HFpEF animal models have been reviewed extensively,[21,45,133-135] we investigated if clinically relevant HFpEF phenogroups could be implemented into a tool to guide selection of HFpEF animal models and better define animal research.

Translating HFpEF phenotypes into animal models remains a difficult process, as both the developing triggers and the diagnostic approaches are different between humans and animals. Some models from all 3 phenogroups, eg, the ANGII and db/db mice; the DahlSS/obese, ZSF1/obese, and Fischer 344 rat; and the HT/HC/DM pig, have been used in exercise testing, which reinforces their potential as HFpEF models instead of only extended LVDD models.

Our findings show that by defining phenogroups in animal models, more precise comparisons can be made between animals and specific phenotypically and regionally different patient populations.[23] For future research, our developed scoring system of phenogroups with parameters relevant to animals could prove beneficial for further developing and evaluating effective LVDD/HFpEF animal models. The **Central Illustration** shows the scoring of animal models for their respective phenogroup, to guide the selection of a suitable animal model for your research question. Before conclusions can be drawn, it should be mentioned that many animal models included here should be better defined as extended LVDD animal models, as clinical characteristics of HFpEF are often lacking.

DRAWBACKS AND FUTURE PERSPECTIVES

Animal models for LVDD/HFpEF are almost always initiated by comorbidities, attempting to mimic the progression from LVDD to HF. Acute induction of pressure overload, eg, by transverse aortic constriction (TAC), leads to LVDD in animals within a short time frame, whereas in humans this often is a slow process likely caused by less extreme physiological changes. Although some studies show preserved LVEF in TAC models,[136,137] many also report the development of systolic dysfunction with reduced LVEF within a couple of weeks upon pressure overload.[138-140] In addition, TAC animal models that include multiple comorbidities in parallel also show the greatest reduction in LVEF. These inconsistencies make it difficult to recognize these models as true LVDD/HFpEF models, and further refinement of the model would be required.

To prevent all early-stage HF models from being called LVDD models, we propose to show at least 1 parameter of active and passive relaxation abnormalities, increased diastolic pressure, and tissue adaptations, such as cardiac hypertrophy, to extensively prove LVDD. One hallmark of LVDD/HFpEF in patients is systemic inflammation, which should also be crucial characteristic in animal models. It can also act as an important therapeutic target, eg, as shown in the CANTOS trial,[13,141] and is associated with comorbidities.[142] In addition to LVDD parameters, an assessment of inflammatory state, such as amount of circulating inflammatory cells and/or cytokines and chemokines, is also recommended. Moreover, the described parameters for LVDD/HFpEF comorbidities should be investigated, where our clustering can aid in selection.

Until now, a translational gap between animal models and clinical LVDD/HFpEF has remained, as HFpEF is an incompletely understood and heterogeneous syndrome. Importantly, it has become clear that cardiac amyloidosis may be present in 10%-15% of patients diagnosed with HFpEF, which could have a significant impact on HFpEF heterogeneity and outcome in HFpEF trials.[143,144] Although other comorbidities of HFpEF, such as atrial fibrillation and chronic obstructive pulmonary disease, are also recognized in patients, to the best of our knowledge no animal models showing these characteristics have been created so far. Therefore, we evaluated only the 4 most pronounced mentioned comorbidities.

Also, elevated BNP or other clinically relevant biomarkers, such as growth/differentiation factor 15, could provide more insights into phenogroups,

CENTRAL ILLUSTRATION Selection-Guide for Animals Models of HFpEF Based on Clinical Phenogroups
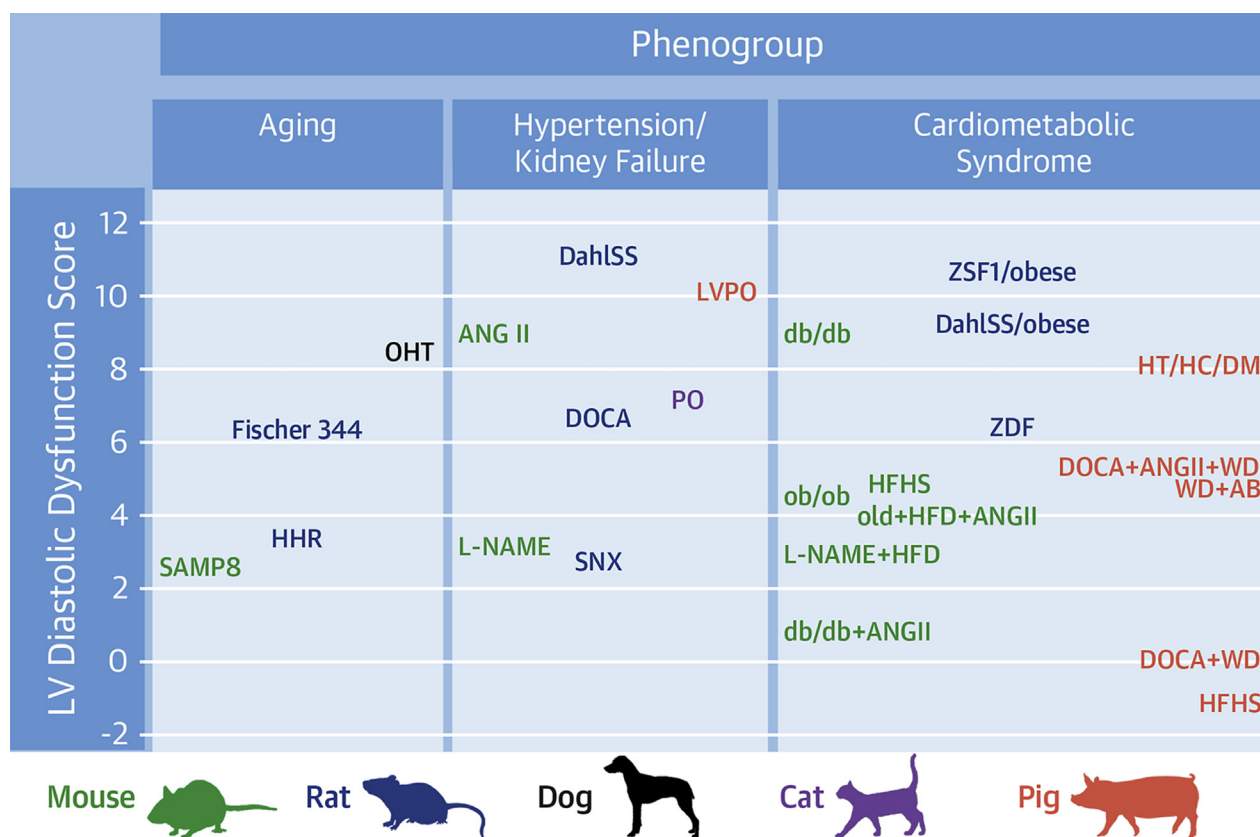
van Ham WB, et al. J Am Coll Cardiol Basic Trans Science. 2022;7(8):844–857.

A tool to help selection of suitable animal models for underlying phenogroups based on their scoring explained in this paper. Three phenogroups were translated from applicable clinical phenogroups into preclinical animal models: aging, hypertension/kidney failure, and cardiometabolic syndrome. **Colors** represent different model animals (from small on the **left** to big on the **right**). The higher a model is on the scale, the more suitable it is to mimic the phenogroup. AB = aortic block pig; ANG II = angiotensin II; DahlSS = Dahl salt sensitive; db/db = diabetic mouse; DOCA = deoxycorticosterone acetate rat; HFD = high fat diet mouse; HFHS = high-fat, high-sugar pig; HHR = hypertrophic heart rat; HT/HC/DM = hypertensive; hypercholesterolemia diabetes mellitus pig; L-NAME = Nω-nitrol-argininemethyl ester; LVPO = left ventricular pressure overload; ob/ob = obese mouse; OHT = old hypertensive dog; PO = pressure overload; SAMP8 = senescence-accelerated mouse prone 8 mouse; SNX = subtotal nephrectomy rat; WD = Western Diet pig; ZSF1 = Zucker fatty and spontaneously hypertensive.

because different phenogroups correlate with different BNP levels.[16-19] However, BNP was only investigated in approximately one-half of the models. It should be noted that BNP levels are normal in almost one-third of the human HFpEF population; can also be affected by, eg, obesity[145,146]; and are generally lower in women compared with men.[147] Increased growth/differentiation factor 15 expression, although not yet measured in animal models, is increasingly used as a biomarker for inflammation and cell stress, whereas the expression remains relatively low during healthy conditions.[148]

Because HFpEF is more prevalent in women,[11,57,147] female animals should be included in an appropriate ratio to male animals, but so far only few animal studies take sex differences into account, even use female animals, or fail to report on the sex used.[149-151] These studies mainly showed that obesity was more prominent in female compared with male animals, but both sexes had similar functional cardiac outcomes.[116,119,127,128] Some studies did use both sexes but did not stratify their results, thereby possibly omitting valuable data. Detailed differences in disease pathophysiology are yet unknown, and future animal studies should include both sexes as well as stratify all data to investigate possible differences. To substantiate, it was shown that estrogen depletion results in cardiac hypertrophy and

disrupted calcium handling,[152] as well as elevated ROS production, resulting in cardiac fibrosis and microvascular dysfunction.[153,154]

CONCLUSIONS

This review clustered animal models into clinical phenogroups of HFpEF to make preclinical research more focused and translational. We created a grouping method that facilitates the choice of an appropriate animal model based on the phenogroup of interest, and simultaneously scored the models based on the investigated extensiveness of LVDD, systemic inflammation, and fibrosis formation.

Based on our scoring, the most promising animal model from the phenogroup aging is the OHT model, and although clinically aging is an important characteristic, the fast-aging models did not show clear LVDD. The best fitting models from the phenogroup hypertension/kidney dysfunction are the ANGII mouse, the DahlSS rat, and the LVPO pig. For the phenogroup cardiometabolic syndrome, the db/db mouse develops obesity and T2DM without hypertension and is showing LVDD. Also, the DahlSS/obese and ZSF1/obese rat and the HT/HC/DM pig models had good overall scores and stand out with HF marker and sex reports. Despite lower scores, the DOCA + ANGII + WD and the WD + AB pig models are the most suitable large animal models, as LVDD is proven most extensively.

In the future, this basic clustering can be used to improve missing aspects of a model and be adapted accordingly.

ADDRESS FOR CORRESPONDENCE: Dr Saskia C.A. de Jager, Laboratory for Experimental Cardiology, Department of Cardiology, University Medical Center Utrecht, Heidelberglaan 100, Utrecht 3584 CX, the Netherlands. E-mail: S.C.A.deJager@umcutrecht.nl.

REFERENCES

1. Borlaug B, Paulus W. Heart failure with preserved ejection fraction: pathophysiology, diagnosis, and treatment. *Eur Heart J.* 2011;32(6): 670–679.

2. Lam C, Donal E, Kraigher-Krainer E, Vasan R. Epidemiology and clinical course of heart failure with preserved ejection fraction. *Eur J Heart Fail.* 2014;13(1):18–28.

3. Pandey A, Patel K, Vaduganathan M, et al. Physical activity, fitness, and obesity in heart failure with preserved ejection fraction. *J Am Coll Cardiol HF.* 2018;6(12):975–982.

4. Streng K, Nauta J, Hillege H, et al. Non-cardiac comorbidities in heart failure with reduced, mid-range and preserved ejection fraction. *Int J Cardiol.* 2018;271:132–139.

5. Tibrewala A, Yancy C. Heart failure with preserved ejection fraction in women. *Heart Fail Clin.* 2019;15(1):9–18.

6. Andersson C, Vasan R. Epidemiology of heart failure with preserved ejection fraction. *Heart Fail Clin.* 2014;10(3):377–388.

7. Ponikowski P, Voors A, Anker S, et al. 2016 ESC Guidelines for the diagnosis and treatment of acute and chronic heart failure. *Eur Heart J.* 2016;37:2129–2200.

8. Kovács Á, Papp Z, Nagy L. Causes and pathophysiology of heart failure with preserved ejection fraction. *Heart Fail Clin.* 2014;10:389–398.

9. Simmonds S, Cuijpers I, Heymans S, Jones E. Cellular and molecular differences between HFpEF and HFrEF: a step ahead in an improved pathological understanding. *Cells.* 2020;9(1): E242.

10. Dunlay S, Roger V, Redfield M. Epidemiology of heart failure with preserved ejection fraction. *Nat Rev Cardiol.* 2017;14(10):591–602.

11. Goyal P, Paul T, Almarzooq Z, et al. Sex- and race-related differences in characteristics and outcomes of hospitalizations for heart failure with preserved ejection fraction. *J Am Heart Assoc.* 2017;6(4):1–10.

12. Sorop O, Heinonen I, Kranenburg M, et al. Multiple common comorbidities produce left ventricular diastolic dysfunction associated with coronary microvascular dysfunction, oxidative stress, and myocardial stiffening. *Cardiovasc Res.* 2018;114(7):954–964.

13. Kessler E, Oerlemans M, Van den Hoogen P, Yap C, Sluijter J, De Jager S. Immunomodulation in heart failure with preserved ejection fraction: current state and future perspectives. *J Cardiovasc Transl Res.* 2020;14:63–74.

14. Reddy Y, Carter R, Obokata M, Redfield M, Borlaug B. A simple, evidence-based approach to help guide diagnosis of heart failure with preserved ejection fraction. *Circulation.* 2018;138(9): 861–870.

15. Pieske B, Tschöpe C, De Boer R, et al. How to diagnose heart failure with preserved ejection fraction: the HFA-PEFF diagnostic algorithm: a consensus recommendation from the Heart Failure Association (HFA) of the European Society of Cardiology (ESC). *Eur Heart J.* 2019;40(40):3297–3317.

16. Gu J, Pan JA, Lin H, Zhang JF, Wang CQ. Characteristics, prognosis and treatment response in distinct phenogroups of heart failure with preserved ejection fraction. *Int J Cardiol.* 2021;323: 148–154.

17. Shah S, Katz D, Selvaraj S, et al. Phenomapping for novel classification of heart failure with preserved ejection fraction. *Circulation.* 2015;131(3): 269–279.

18. Cohen J, Schrauben S, Zhao L, et al. Clinical phenogroups in heart failure with preserved ejection fraction: detailed phenotypes, prognosis, and response to spironolactone. *J Am Coll Cardiol. HF.* 2020;8(3):172–184.

19. Segar M, Patel K, Ayers C, et al. Phenomapping of patients with heart failure with preserved ejection fraction using machine learning-based unsupervised cluster analysis. *Eur J Heart Fail.* 2020;22(1):148–158.

20. Vaduganathan M, Patel R, Michel A, et al. Mode of death in heart failure with preserved ejection fraction. *J Am Coll Cardiol.* 2017;69(5): 556–569.

21. Horgan S, Watson C, Glezeva N, Baugh J. Murine models of diastolic dysfunction and heart failure with preserved ejection fraction. *J Card Fail.* 2014;20(12):984–995.

22. Withaar C, Lam CSP, Schiattarella GG, de Boer RA, Meems LMG. Heart failure with preserved ejection fraction in humans and mice: embracing clinical complexity in mouse models. *Eur Heart J.* 2021;42(43):4420–4430.

23. Solomon S, Rizkala A, Lefkowitz M, et al. Baseline characteristics of patients with heart failure and preserved ejection fraction in the PARAGON-HF Trial. *Circ Heart Fail.* 2018;11(7):1–10.

24. Reddy Y, Borlaug B. Heart failure with preserved ejection fraction. *Curr Probl Cardiol.* 2016;41(4):145–188.

25. Kotecha D, Lam C, Van Veldhuisen D, Van Gelder I, Voors A, Rienstra M. Heart failure with preserved ejection fraction and atrial fibrillation: vicious twins. *J Am Coll Cardiol.* 2016;68(20): 2217–2228.

26. Maurer M, Spevack D, Burkhoff D, Kronzon I. Diastolic dysfunction: can it be diagnosed by doppler echocardiography? *J Am Coll Cardiol.* 2004;44(8):1543–1549.

27. Lee S, Park M, Park Y, Lee S. E/E' ratio is more sensitive than E/A ratio for detection of left ventricular diastolic dysfunction in systemic lupus erythematosus. *Lupus.* 2008;17(5):195–201.

28. Zile M, Baicu C, Gaasch W. Diastolic heart failure — abnormalities in active relaxation and passive stiffness of the left ventricle. *N Engl J Med.* 2004;350:1953–1959.

29. Van den Dorpel M, Heinonen I, Snelder S, et al. Early detection of left ventricular diastolic dysfunction using conventional and speckle tracking echocardiography in a large animal model of metabolic dysfunction. *Int J Cardiovasc Imaging.* 2018;34(5):743–749.

30. LaPointe M. Molecular regulation of the brain natriuretic peptide gene. *Peptides.* 2005;26(6): 944–956.

31. Thomas L, Marwick T, Popescu B, Donal E, Badano L. Left atrial structure and function, and left ventricular diastolic dysfunction: JACC state-of-the-art review. *J Am Coll Cardiol.* 2019;73(15): 1961–1977.

32. Paulus W, Tschöpe C. A novel paradigm for heart failure with preserved ejection fraction: Comorbidities drive myocardial dysfunction and remodeling through coronary microvascular endothelial inflammation. *J Am Coll Cardiol.* 2013;62(4):263–271.

33. Packer M, Lam C, Lund L, Maurer M, Borlaug B. Characterization of the inflammatory-metabolic phenotype of heart failure with a preserved ejection fraction: a hypothesis to explain influence of sex on the evolution and potential treatment of the disease. *Eur J Heart Fail.* 2020;22(9):1551–1567.

34. Westermann D, Lindner D, Kasner M, et al. Cardiac inflammation contributes to changes in the extracellular matrix in patients with heart failure and normal ejection fraction. *Circ Heart Fail.* 2011;4(1):44–52.

35. DuBrock H, AbouEzzeddine O, Redfield M. High-sensitivity C-reactive protein in heart failure with preserved ejection fraction. *PLoS One.* 2018;13(8):e0201836.

36. Michels da Silva D, Langer H, Graf T. Inflammatory and molecular pathways in heart failure—ischemia, HFpEF and transthyretin cardiac amyloidosis. *Int J Mol Sci.* 2019;20(9):2322.

37. Mohammed S, Hussain S, Mirzoyev S, Edwards W, Maleszewski J, Redfield M. Coronary microvascular rarefaction and myocardial fibrosis in heart failure with preserved ejection fraction. *Circulation.* 2015;131(6):550–559.

38. Hamilton-Craig C, Strudwick M, Galloway G. T1 mapping for myocardial fibrosis by cardiac magnetic resonance relaxometry—a comprehensive technical review. *Front Cardiovasc Med.* 2016;3: 49.

39. López B, González A, Díez J. Circulating biomarkers of collagen metabolism in cardiac diseases. *Circulation.* 2010;121(14):1645–1654.

40. Collier P, Watson C, Voon V, et al. Can emerging biomarkers of myocardial remodelling identify asymptomatic hypertensive patients at risk for diastolic dysfunction and diastolic heart failure? *Eur J Heart Fail.* 2011;13(10):1087–1095.

41. Michalska-Kasiczak M, Bielecka-Dabrowa A, Von Haehling S, Anker S, Rysz J, Banach M. Biomarkers, myocardial fibrosis and co-morbidities in heart failure with preserved ejection fraction: an overview. *Arch Med Sci.* 2018;14(4):890–909.

42. De Jong S, Van Veen T, De Bakker J, Vos M, Van Rijen H. Biomarkers of myocardial fibrosis. *J Cardiovasc Pharmacol.* 2011;57(5):522–535.

43. Bielecka-Dabrowa A, Sakowicz A, Misztal M, et al. Differences in biochemical and genetic biomarkers in patients with heart failure of various etiologies. *Int J Cardiol.* 2016;221:1073–1080.

44. Poole D, Copp S, Colburn T, et al. Guidelines for animal exercise and training protocols for cardiovascular studies. *Am J Physiol Heart Circ Physiol.* 2020;318(5):H1100–H1138.

45. Valero-Muñoz M, Backman W, Sam F. Murine models of heart failure with preserved ejection fraction: a "fishing expedition.". *J Am Coll Cardiol Basic Trans Science.* 2017;2(6):770–789.

46. Kao D, Lewsey J, Anand I, et al. Characterization of subgroups of heart failure patients with preserved ejection fraction with possible implications for prognosis and treatment response. *Eur J Heart Fail.* 2015;17(9):925–935.

47. Kaptein Y, Karagodin I, Zuo H, et al. Identifying phenogroups in patients with subclinical diastolic dysfunction using unsupervised statistical learning. *BMC Cardiovasc Disord.* 2020;20(1): 367.

48. Katz D, Deo R, Aguilar F, et al. Phenomapping for the identification of hypertensive patients with the myocardial substrate for heart failure with preserved ejection fraction. *J Cardiovasc Transl Res.* 2017;10:275–284.

49. Uijl A, Savarese G, Vaartjes I, et al. Identification of distinct phenotypic clusters in heart failure with preserved ejection fraction. *Eur J Heart Fail.* 2021;23(6):973–982.

50. Woolley RJ, Ceelen D, Ouwerkerk W, et al. Machine learning based on biomarker profiles identifies distinct subgroups of heart failure with preserved ejection fraction. *Eur J Heart Fail.* 2021;23(6):983–991.

51. Karuppagounder V, Arumugam S, Babu S, et al. The senescence accelerated mouse prone 8 (SAMP8): A novel murine model for cardiac aging. *Ageing Res Rev.* 2016;35:291–296.

52. Reed A, Tanaka A, Sorescu D, et al. Diastolic dysfunction is associated with cardiac fibrosis in the senescence-accelerated mouse. *Am J Physiol Circ Physiol.* 2011;301(3):H824–H831.

53. Bustamante M, Garate-Carrillo A, Ito B, et al. Unmasking of oestrogen-dependent changes in left ventricular structure and function in aged female rats: a potential model for pre-heart failure with preserved ejection fraction. *J Physiol.* 2019;597(7):1805–1817.

54. Loredo-Mendoza M, Ramirez-Sanchez I, Bustamante-Pozo M, et al. The role of inflammation in driving left ventricular remodeling in a pre-HFpEF model. *Exp Biol Med.* 2020;245(8):748–757.

55. Curl CL, Danes VR, Bell JR, et al. Cardiomyocyte functional etiology in heart failure with preserved ejection fraction is distinctive-a new preclinical model. *J Am Heart Assoc.* 2018;7(11):1–13.

56. Shah S, Lam C, Svedlund S, et al. Prevalence and correlates of coronary microvascular dysfunction in heart failure with preserved ejection fraction: PROMIS-HFpEF. *Eur Heart J.* 2018;39(37):3439–3450.

57. Hoshida S, Watanabe T, Shinoda Y, et al. Sex-related differences in left ventricular diastolic function and arterial elastance during admission in patients with heart failure with preserved ejection fraction: the PURSUIT HFpEF study. *Clin Cardiol.* 2018;8:1–8.

58. Gori M, Lam C, Gupta D, et al. Sex-specific cardiovascular structure and function in heart failure with preserved ejection fraction. *Eur J Heart Fail.* 2014;16(5):535–542.

59. Lam C, Carson P, Anand I, et al. Sex differences in clinical characteristics and outcomes in elderly patients with heart failure and preserved ejection fraction: the Irbesartan in Heart Failure with Preserved Ejection Fraction (I-PRESERVE) trial. *Circ Heart Fail.* 2012;5(5):571–578.

60. Ruiz-Ortega M, Esteban V, Rupérez M, et al. Renal and vascular hypertension-induced inflammation: role of angiotensin II. *Nephrol Hypertens.* 2006;15(2):159–166.

61. Dryer K, Gajjar M, Narang N, et al. Coronary microvascular dysfunction in patients with heart failure with preserved ejection fraction. *Am J Physiol Circ Physiol.* 2018;314(5):H1033–H1042.

62. Hamdani N, Franssen C, Lourenço A, et al. Myocardial titin hypophosphorylation importantly contributes to heart failure with preserved ejection fraction in a rat metabolic risk model. *Circ Heart Fail.* 2013;6(6):1239–1249.

63. Mattson D. Comparison of arterial blood pressure in different strains of mice. *Am J Hypertens.* 2001;14(5):405–408.

64. Zhao X, Ho D, Gao S, Hong C, Vatner D, Vatner S. Arterial pressure monitoring in mice. *Curr Protoc Mouse Biol*. 2011;1(1):105–122.

65. Buñag R, Teräväinen T. Tail-cuff detection of systolic hypertension in different strains of ageing rats. *Mech Aging Dev*. 1991;59(1-2):197–213.

66. Duca F, Zotter-Tufaro C, Kammerlander AA, et al. Gender-related differences in heart failure with preserved ejection fraction. *Sci Rep*. 2018;8(1):1–9.

67. Pei J, Harakalova M, den Ruijter H, et al. Cardiorenal disease connection during postmenopause: the protective role of estrogen in uremic toxins induced microvascular dysfunction. *Int J Cardiol*. 2017;238:22–30.

68. Gorin Y, Block K. Nox as a Target for diabetic complications. *Clin Sci*. 2013;125(8):361–382.

69. You Y, Okada S, Ly S, et al. Role of Nox2 in diabetic kidney disease. *Am J Physiol Physiol*. 2013;304(7):840–848.

70. Van Dijk C, Oosterhuis N, Xu Y, et al. Distinct endothelial cell responses in the heart and kidney microvasculature characterize the progression of heart failure with preserved ejection fraction in the obese ZSF1 rat with cardiorenal metabolic syndrome. *Circ Heart Fail*. 2016;9(4):1–13.

71. Schwarzl M, Hamdani N, Seiler S, et al. A porcine model of hypertensive cardiomyopathy: implications for heart failure with preserved ejection fraction. *Am J Physiol Heart Circ Physiol*. 2015;309(9):H1407–H1418.

72. Hattori T, Murase T, Ohtake M, et al. Characterization of a new animal model of metabolic syndrome: the DahlS.Z-Lepr(fa)/Lepr(fa)rat. *Nutr Diabetes*. 2011;1:1–6.

73. Gava A, Freitas F, Balarini C, Vasquez E, Meyrelles S. Effects of 5/6 nephrectomy on renal function and blood pressure in mice. *Int J Physiol Pathophysiol Pharmacol*. 2012;4(3):167–173.

74. Baracho N, Kangussu L, Prestes T, et al. Characterization of an experimental model of progressive renal disease in rats. *Acta Cir Bras*. 2016;31(11):744–752.

75. Jang M, Son WG, Jo SM, Kim H, Shin CW, Lee I. Effect of intra-abdominal hypertension on plasma exogenous creatinine clearance in conscious and anesthetized dogs. *J Vet Emerg Crit Care*. 2019;29(4):366–372.

76. Qureshi S, Patel N, Murphy G. Vascular endothelial cell changes in postcardiac surgery acute kidney injury. *Am J Physiol Physiol*. 2018;314(5): F726–F735.

77. Falcão-Pires I, Hamdani N, Borbély A, et al. Diabetes mellitus worsens diastolic left ventricular dysfunction in aortic stenosis through altered myocardial structure and cardiomyocyte stiffness. *Circulation*. 2011;124(10):1151–1159.

78. McHugh K, DeVore A, Wu J, et al. Heart failure with preserved ejection fraction and diabetes: JACC state-of-the-art review. *J Am Coll Cardiol*. 2019;73(5):602–611.

79. Obokata M, Reddy Y, Pislaru S, Melenovsky V, Borlaug B. Evidence supporting the existence of a distinct obese phenotype of heart failure with preserved ejection fraction. *Circulation*. 2017;136(1):6–19.

80. Van Heerebeek L, Hamdani N, Falcão-Pires I, et al. Low myocardial protein kinase G activity in heart failure with preserved ejection fraction. *Circulation*. 2012;126(7):830–839.

81. Yin W, Carballo-Jane E, McLaren D, et al. Plasma lipid profiling across species for the identification of optimal animal models of human dyslipidemia. *J Lipid Res*. 2012;53(1):51–65.

82. Sun C, Li X, Liu L, et al. Effect of fasting time on measuring mouse blood glucose level. *Int J Clin Exp Med*. 2016;9(2):4186–4189.

83. Wang Z, Yang Y, Xiang X, Zhu Y, Men J, He M. Estimation of the normal range of blood glucose in rats. *Wei Sheng Yan Jiu*. 2010;39(2):133–137.

84. American Diabetes Association. Screening for type 2 diabetes. *Clin Diabetes*. 2000;18(2):69.

85. Bellinger D, Merricks E, Nichols T. Swine models of type 2 diabetes mellitus: insulin resistance, glucose tolerance, and cardiovascular complications. *Inst Lab Anim Res J*. 2006;47(3): 243–258.

86. Mattheeuws D, Rottiers R, Kaneko J, Vermeulen A. Diabetes mellitus in dogs: relationship of obesity to glucose tolerance and insulin response. *Am J Vet Res*. 1984;45(1):98–103.

87. Duprez D, Gross M, Kizer J, Ix J, Hundley W, Jacobs D. Predictive value of collagen biomarkers for heart failure with and without preserved ejection fraction: MESA (Multi-Ethnic Study of Atherosclerosis). *J Am Heart Assoc*. 2018;7(5): e007885.

88. Shapiro B, Lam C, Patel J, et al. Acute and chronic ventricular-arterial coupling in systole and diastole: Insights from an elderly hypertensive model. *Hypertension*. 2007;50(3):503–511.

89. Zakeri R, Moulay G, Chai Q, et al. Left atrial remodeling and atrioventricular coupling in a canine model of early heart failure with preserved ejection fraction. *Circ Heart Fail*. 2016;9(10): e003238.

90. Hamdani N, Bishu K, von Frieling-Salewsky M, Redfield M, Linke W. Deranged myofilament phosphorylation and function in experimental heart failure with preserved ejection fraction. *Cardiovasc Res*. 2013;97(3):464–471.

91. Munagala V, Hart C, Burnett J, Meyer DM, Redfield MM. Ventricular structure and function in aged dogs with renal hypertension. *Circulation*. 2005;111(9):1128–1135.

92. Torres W, Barlow S, Moore A, et al. Changes in myocardial microstructure and mechanics with progressive left ventricular pressure overload. *J Am Coll Cardiol Basic Trans Science*. 2020;5(5): 463–480.

93. Yarbrough W, Mukherjee R, Stroud R, et al. Progressive induction of left ventricular pressure overload in a large animal model elicits myocardial remodeling and a unique matrix signature. *J Thorac Cardiovasc Surg*. 2012;143(1):215–223.

94. Tan W, Li X, Zheng S, Li X, et al. A porcine model of heart failure with preserved ejection fraction induced by chronic pressure overload characterized by cardiac fibrosis and remodeling. *Front Cardiovasc Med*. 2021;8:677727.

95. Wallner M, Eaton D, Berretta R, et al. A Feline HFpEF model with pulmonary hypertension and compromised pulmonary function. *Sci Rep*. 2017;7(1):1–13.

96. Wallner M, Eaton D, Berretta R, et al. HDAC inhibition improves cardiopulmonary function in a feline model of diastolic dysfunction. *Sci Transl Med*. 2020;12(525):eaay7205.

97. Choi Y, De Mattos A, Shao D, et al. Preservation of myocardial fatty acid oxidation prevents diastolic dysfunction in mice subjected to angiotensin II infusion. *J Mol Cell Cardiol*. 2016;100:64–71.

98. Murdoch C, Chaubey S, Zeng L, et al. Endothelial NADPH oxidase-2 promotes interstitial cardiac fibrosis and diastolic dysfunction through proinflammatory effects and endothelial- mesenchymal transition. *J Am Coll Cardiol*. 2014;63(24): 2734–2741.

99. Regan J, Mauro A, Carbone S, et al. A mouse model of heart failure with preserved ejection fraction caused by chronic infusion of a low subpressor dose of angiotensin II. *Am J Physiol Heart Circ Physiol*. 2015;309:H771–H778.

100. Zhong Y, Tang R, Lu Y, et al. Irbesartan may relieve renal injury by suppressing Th22 cells chemotaxis and infiltration in Ang II-induced hypertension. *Int Immunopharmacol*. 2020;87: 106789.

101. Doi R, Masuyama T, Yamamoto K, et al. Development of different phenotypes of hypertensive heart failure: systolic versus diastolic failure in Dahl salt-sensitive rats. *J Hypertens*. 2000;18(1):111–120.

102. Zhang W, Zhang H, Yao W, Li L, Niu P, Huo Y, et al. Morphometric, hemodynamic, and multiomics analyses in heart failure rats with preserved ejection fraction. *Int J Mol Sci*. 2020;21(9): E3362.

103. Omori Y, Ohtani T, Sakata Y, et al. L-carnitine prevents the development of ventricular fibrosis and heart failure with preserved ejection fraction in hypertensive heart disease. *J Hypertens*. 2012;30(9):1834–1844.

104. Elkholey K, Morris L, Niewiadomska M, et al. Sex differences in the incidence and mode of death in rats with heart failure with preserved ejection fraction. *Exp Physiol*. 2021;106(3):673–682.

105. Schiattarella G, Altamirano F, Tong D, et al. Nitrosative stress drives heart failure with preserved ejection fraction. *Nature*. 2019;568(7752): 351–356.

106. Fanelli C, Dellê H, Cavaglieri R, Dominguez W, Noronha I. Gender differences in the progression of experimental chronic kidney disease induced by chronic nitric oxide inhibition. *Biomed Res Int*. 2017;2017:2159739.

107. Bongartz L, Joles J, Verhaar M, et al. Subtotal nephrectomy plus coronary ligation leads to more pronounced damage in both organs than either nephrectomy or coronary ligation. *Am J Physiol Heart Circ Physiol*. 2012;302:H845–H854.

108. Lekawanvijit S, Kompa A, Manabe M, et al. Chronic kidney disease-induced cardiac fibrosis is ameliorated by reducing circulating levels of a non-dialysable uremic toxin, indoxyl sulfate. *PLoS One*. 2012;7(7):e41281.

109. Grobe J, Mecca A, Mao H, Katovich M. Chronic angiotensin- (1-7) prevents cardiac fibrosis in DOCA-salt model of hypertension. *Am J Physiol Heart Circ Physiol*. 2006;290(1):H2417–H2423.

110. Amara V, Surapaneni S, Tikoo K. Metformin attenuates cardiovascular and renal injury in uninephrectomized rats on DOCA-salt: involvement of AMPK and miRNAs in cardioprotection. *Toxicol Appl Pharmacol*. 2019;362:95–104.

111. Allan A, Fenning A, Levick S, Hoey A, Brown L. Reversal of cardiac dysfunction by selective ET-A receptor antagonism. *Br J Pharmacol*. 2005;146(6):846–853.

112. Radovits T, Korkmaz S, Mátyás C, et al. An altered pattern of myocardial histopathological and molecular changes underlies the different characteristics of type-1 and type-2 diabetic cardiac dysfunction. *J Diabetes Res*. 2015;728741.

113. Steven S, Oelze M, Hanf A, et al. The SGLT2 inhibitor empagliflozin improves the primary diabetic complications in ZDF rats. *Redox Biol*. 2017;13:370–385.

114. Mátyás C, Németh B, Oláh A, et al. Prevention of the development of heart failure with preserved ejection fraction by the phosphodiesterase-5A inhibitor vardenafil in rats with type 2 diabetes. *Eur J Heart Fail*. 2017;19(3):326–336.

115. Van Den Bergh A, Vanderper A, Vangheluwe P, et al. Dyslipidaemia in type II diabetic mice does not aggravate contractile impairment but increases ventricular stiffness. *Cardiovasc Res*. 2008;77(2):371–379.

116. Sartori M, Conti F, da Silva Dias D, et al. Association between diastolic dysfunction with inflammation and oxidative stress in females ob/ob mice. *Front Physiol*. 2017;23(8):572.

117. Christoffersen C, Bollano E, Lindegaard M, et al. Cardiac lipid accumulation associated with diastolic dysfunction in obese mice. *Endocrinology*. 2003;144(8):3483–3490.

118. Dong F, Zhang X, Yang X, et al. Impaired cardiac contractile function in ventricular myocytes from leptin-deficient ob/ob obese mice. *J Endocrinol*. 2006;188(1):25–36.

119. Alex L, Russo I, Holoborodko V, Frangogiannis N. Characterization of a mouse model of obesity-related fibrotic cardiomyopathy that recapitulates features of human heart failure with preserved ejection fraction. *Am J Physiol Circ Physiol*. 2018;315(4):H934–H949.

120. Mori J, Patel V, Abo Alrob O, et al. Angiotensin 1-7 ameliorates diabetic cardiomyopathy and diastolic dysfunction in db/db mice by reducing lipotoxicity and inflammation. *Circ Heart Fail*. 2014;7(2):327–339.

121. Broderick T, Sennott J, Gutkowska J, Jankowski M. Anti-inflammatory and angiogenic effects of exercise training in cardiac muscle of diabetic mice. *Diabetes Metab Syndr Obes*. 2019;12:565–573.

122. Alawi L, Emberesh S, Owuor B, et al. Effect of hyperglycemia and rosiglitazone on renal and urinary neprilysin in db/db diabetic mice. *Physiol Rep*. 2020;8(3):e14364.

123. Aboumsallem K, Muthuramu I, Mishra M, Kempen H, De Geest B. Effective treatment of diabetic cardiomyopathy and heart failure with reconstituted HDL (Milano) in mice. *Int J Mol Sci*. 2019;20(6):1273.

124. Withaar C, Meems L, Markousis-Mavrogenis G, et al. The effects of liraglutide and dapagliflozin on cardiac function and structure in a multi-hit mouse model of Heart Failure with Preserved Ejection Fraction. *Cardiovasc Res*. 2021;117(9):2108–2124.

125. Heinonen I, Sorop O, Van Dalen B, et al. Cellular, mitochondrial and molecular alterations associate with early left ventricular diastolic dysfunction in a porcine model of diabetic metabolic derangement. *Sci Rep*. 2020;10(1):13173.

126. Uchinaka A, Kawashima Y, Sano Y, et al. Effects of ramelteon on cardiac injury and adipose tissue pathology in rats with metabolic syndrome. *Ann N Y Acad Sci*. 2018;1421(1):73–87.

127. Murase T, Hattori T, Ohtake M, et al. Cardiac remodeling and diastolic dysfunction in DahlS.Z-Lepr fa/Lepr fa rats: a new animal model of metabolic syndrome. *Hypertens Res*. 2012;35:186–193.

128. Nguyen I, Brandt M, Van de Wouw J, et al. Both male and female obese ZSF1 Rats develop cardiac dysfunction in obesity-induced heart failure with preserved ejection fraction. *PLoS One*. 2020;15(5):e0232399.

129. Zhang N, Feng B, Ma X, Sun K, Xu G, Zhou Y. Dapagliflozin improves left ventricular remodeling and aorta sympathetic tone in a pig model of heart failure with preserved ejection fraction. *Cardiovasc Diabetol*. 2019;18(1):107.

130. Van de Wouw J, Steenhorst J, Sorop O, et al. Impaired pulmonary vasomotor control in exercising swine with multiple comorbidities. *Basic Res Cardiol*. 2021;116(1):51.

131. Olver T, Edwards J, Jurrissen T, et al. Western diet-fed, aortic-banded ossabaw swine: a preclinical model of cardio-metabolic heart failure. *J Am Coll Cardiol Basic Trans Science*. 2019;4(3):404–421.

132. Van Bilsen M, Daniels A, Brouwers O, et al. Hypertension is a conditional factor for the development of cardiac hypertrophy in type 2 diabetic mice. *PLoS One*. 2014;9(1):e85078.

133. Silva K, Emter C. Large animal models of heart failure: a translational bridge to clinical success. *J Am Coll Cardiol Basic Trans Science*. 2020;5(8):840–856.

134. Riehle C, Bauersachs J. Small animal models of heart failure. *Cardiovasc Res*. 2019;115(13):1838–1849.

135. Conceição G, Heinonen I, Lourenço AP, Duncker DJ, Falcão-Pires I. Animal models of heart failure with preserved ejection fraction. *Netherlands Hear J*. 2016;24(4):275–286.

136. De Jong A, Van Gelder I, Vreeswijk-Baudoin I, Cannon M, Van Gilst W, Maass A. Atrial remodeling is directly related to end-diastolic left ventricular

pressure in a mouse model of ventricular pressure overload. *PLoS One*. 2013;8(9):1–11.

137. Zhou Q, Kesteven S, Wu J, et al. Pressure overload by transverse aortic constriction induces maladaptive hypertrophy in a titin-truncated mouse model. *Biomed Res Int*. 2015;2015:163564.

138. Slater R, Strom J, Methawasin M, et al. Metformin improves diastolic function in an HFpEF-like mouse model by increasing titin compliance. *J Gen Physiol*. 2019;151(1):42–52.

139. Wang J, Fontes M, Wang X, et al. Leukocytic toll-like receptor 2 deficiency preserves cardiac function and reduces fibrosis in sustained pressure overload. *Sci Rep*. 2017;7(1):9193.

140. Kessler E, Wang J, Kok B, et al. Ventricular TLR4 levels abrogate TLR2-mediated adverse cardiac remodeling upon pressure overload in mice. *Int J Mol Sci*. 2021;22(21):11823.

141. Everett B, Cornel J, Lainscak M, et al. Anti-inflammatory therapy with canakinumab for the prevention of hospitalization for heart failure. *Circulation*. 2019;139(10):1289–1299.

142. Sanders-van Wijk S, Tromp J, Beussink-Nelson L, et al. Proteomic evaluation of the comorbidity-inflammation paradigm in heart failure with preserved ejection fraction: results from the PROMIS-HFpEF Study. *Circulation*. 2020;142(21):2029–2044.

143. Oerlemans M, Rutten K, Minnema M, Raymakers R, Asselbergs F, De Jonge N. Cardiac amyloidosis: the need for early diagnosis. *Netherlands Heart J*. 2019;27(11):525–536.

144. Oghina S, Bougouin W, Bézard M, et al. The impact of patients with cardiac amyloidosis in HFpEF trials. *J Am Coll Cardiol HF*. 2021;9(3):169–178.

145. Tanase D, Radu S, Shurbaji S, et al. Natriuretic peptides in heart failure with preserved left ventricular ejection fraction: from molecular evidences to clinical implications. Int. *J Mol Sci*. 2019;20(11):2629.

146. Pfeffer M, Shah A, Borlaug B. Heart failure with preserved ejection fraction in perspective. *Circ Res*. 2019;124(11):1598–1617.

147. Harada E, Mizuno Y, Kugimiya F, et al. Sex differences in heart failure with preserved ejection fraction reflected by B-type natriuretic peptide level. *Am J Med Sci*. 2018;356(4):335–343.

148. Wischhusen J, Melero I, Fridman W. Growth/ differentiation factor-15 (GDF-15): from biomarker to novel targetable immune checkpoint. *Front Immunol*. 2020;11:951.

149. Clayton J, Arnegard M. Taking cardiology clinical trials to the next level: a call to action. *Clin Cardiol*. 2018;41(2):179–184.

150. Taylor A. Heart failure in women. *Curr Heart Fail Rep*. 2015;12(2):187–195.

151. Perrino C, Ferdinandy P, Bøtker H, et al. Improving translational research in sex-specific effects of comorbidities and risk factors in ischemic heart disease and cardioprotection: position paper and recommendations of the ESC Working Group on Cellular Biology of the Heart. *Cardiovasc Res*. 2020;117(2):367–385.

152. Li S, Gupte A. The role of estrogen in cardiac metabolism and diastolic function. *Methodist Debakey Cardiovasc J*. 2017;13(1):4–8.

153. Zhao Z, Wang H, Jessup J, Lindsey S, Chappell M, Groban L. Role of estrogen in diastolic dysfunction. *J Biol Chem*. 2014;306:H628–H640.

154. Sickinghe A, Korporaal S, Den Ruijter H, Kessler E. Estrogen contributions to microvascular dysfunction evolving to heart failure with preserved ejection fraction. *Front Endocrinol (Lausanne)*. 2019;10:442.

KEY WORDS animal models, heart failure with preserved ejection fraction, HFpEF, left ventricular diastolic dysfunction, LVDD, phenogroups

APPENDIX For supplemental tables, please see the online version of this paper.